ISSN 1975-8359(Print) / ISSN 2287-4364(Online)
The Transactions of the Korean Institute of Electrical Engineers Vol. 65, No. 12, pp. 2183~2188, 2016
http://dx.doi.org/10.5370/KIEE.2016.65.12.2183

RSM을 이용한 CVVT용 전동기 코깅토크 저감 설계

Cogging Torque Reduction Design for CVVT Using Response Surface Methodology

김 재 의* · 김 동 민* · 박 수 환* · 홍 정 표†
(Jae-Yui Kim · Dong-min Kim · Soo-Hwan Park · Jung-Pyo Hong)

Abstract - This paper deals with the design process for an outer-rotor-type surface-mounted permanent magnet synchronous motor (SPMSM) used in continuous variable valve timing (CVVT) systems in automobiles with internal combustion engines. When the same size, outer-rotor-type SPMSMs generate larger torque and more stable than inner-rotor-type SPMSMs. For the initial design, space harmonic analysis (SHA) is used. In order to minimize the cogging torque, an optimization was conducted using Response Surface Methodology (RSM). At the end of the paper, Finite Element Analysis (FEA) is performed to verify the performance of the optimum model.

Key Words : Cogging torque, Optimum design, Space harmonic analysis, Surface-mounted permanent magnet synchronous motor, Response Surface Methodology.

1. Introduction

Eco-friendliness has become a significant issue in the automotive industry. Over 90% of air pollution is the result of vehicle emissions in large cities. The European Union (EU) has strict exhaust emissions laws to protect the environment. In addition, the Corporate Average Fuel Economy (CAFE) in the United States regulates the average fuel mileage for automobile makers through emission policies. Therefore, automobile companies are developing new technologies to meet these environmental regulations. Vehicle engine electrification is one of those strategies.

Two types of engine electrification are currently underway. The first type changes the entire engine from an internal combustion engine to an electric motor for HEVs or EVs. The second type replaces some mechanical components with electric components in the internal combustion engine. In the second case, the sensor, ECU, and actuator are core parts. This paper focus on the actuator, specifically in electric motors, for engine valves.

Valves in an internal combustion engine control the flow of intake and exhaust gases. The timing of the valves lifting and duration largely influences the performance of the engine. In the case of existing mechanical control, valves depend on the quantity of airflow and a fixed compressed ratio. Ignition timing in a chamber is the same as compression process timing. However, the optimum ignition timing of the engine changes continuously owing to the quantity of oxygen, air/fuel ratio, compressed ratio, driving conditions, and so on. Therefore, the valve-timing system of the vehicle is inaccurate. As a result, the engine performs inefficiently, and increasing CO2 and NOx (nitrogen oxide) emission problems occur [1].

By contrast, Continuous Variable Valve Timing (CVVT) continuously controls the timing of the opening and closing of an engine chamber's valves by using an electric motor. In other words, CVVT can control the optimum operating timing of a valve according to engine speed and driving conditions. Therefore, a proper electric motor is essential for stable CVVT operation. Usually an outer-rotor-type SPMSM is used as a CVVT system because it creates higher torque than an inner-rotor type at the same size and is more stable for magnet scattering.

In this paper, an outer-rotor-type SPMSM for CVVT is designed. The Space Harmonic Analysis (SHA) method is used to create the initial design. Initial design points are set by conducting a tendency analysis of phase back EMF, THD, and the cogging torque through SHA. An optimum design method is used to minimize the cogging torque of the initial model. Response Surface Methodology (RSM) with two design variables is conducted. After optimizing, phase back EMF, THD, and cogging torque are calculated by Finite Element Analysis (FEA) to verify the optimum model.

† Corresponding Author : Dept. of Automotive Engineering, Hanyang University, Korea
E-mail : hongjp@hanyang.ac.kr
∗ Dept. of Automotive Engineering, Hanyang University, Korea
Received : October 19, 2016; Accepted : November 28, 2016

Table 1 Specification of the motor

Specification	Content
Type	Outer Rotor SPM
DC link Voltage [V]	12
Pole/Slot number	8/12
Operation type	BLDC 6-step
Rotor outer diameter [mm]	40
Stack length [mm]	23
Cogging torque [Nm]	Max 0.05
Air gap [mm]	0.5
PM residual induction [T]	0.44

2. Initial Design

An outer-rotor-type SPMSM has several merits. First, at the same size, an outer-rotor-type SPMSM generates more torque than an inner-type SPMSM because of the former's longer rotor diameter. Second, a Permanent Magnet (PM) is attached to the inner yoke of the rotor. This means PM scattering is prevented. Third, the housing of the outer-rotor-type SPMSM can be directly used as a gear. Therefore, the engine does not need additional gearboxes, so the outer-rotor-type SPMSM is good for space application side. Specifications for the outer-rotor-type SPMSM are listed in Table 1.

To design outer-rotor-type SPMSM for CVVT, an adequate phase back EMF and minimum cogging torque are required. The initial model design will be achieved by using a numerical analysis method called Space Harmonic Analysis.

2.1 Space Harmonic Analysis

To use the Space Harmonic Analysis method, the magnetic flux density is needed. Magnetic flux density in an air gap is calculated by combining two magnetic fields that are created by PMs and an armature current, respectively. The following assumptions are needed to use SHA:

(a) The permeability of the magnetic core is infinite.
(b) The saturation effect is not considered.
(c) The end effect and eddy current are neglected.
(d) Linear demagnetization characteristics are used.

Fig. 1 (a) shows the magnetic field owing to the PMs. It is divided into four regions. In Fig. 1 (b), the PMs are represented by the Equivalent Magnetizing Current (EMC). Governing equations for each region are as follows [2]:

$$\frac{\partial A(x,y)}{\partial x^2}+\frac{\partial A(x,y)}{\partial y^2}=0 \qquad \text{Region I, II, IV} \qquad (1)$$

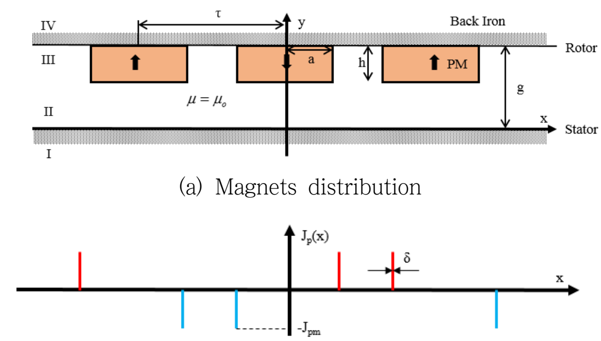

(a) Magnets distribution

(b) Equivalent magnetizing current of magnets

Fig. 1 Magnetic field due to PM

$$\frac{\partial A(x,y)}{\partial x^2}+\frac{\partial A(x,y)}{\partial y^2}=-\mu_0 J_P(x) \qquad \text{Region III} \qquad (2)$$

where A is the z-axis component of the magnetic vector potential, and J_{pm} is the current density of the PMs. The EMC distribution of the PMs is $J_p(x)$, which is expressed as a Fourier series:

$$J_P(x)=\sum_{n=1,3}^{\infty} b_{pn}\cdot\sin(nkx) \qquad (3)$$

$$\text{where, } b_{pn}=\frac{4J_{pm}}{n\pi}[\cos(nka)-\cos nk(a+\delta)], \quad k=\frac{\pi}{\tau} \qquad (4)$$

$$J_{pm}=\frac{\oint \vec{M}\cdot d\vec{l}}{\delta\times h}=\frac{M}{\delta}=\frac{B_r}{\mu_0\delta} \qquad (5)$$

where δ indicates an arbitrary value that approaches zero, and magnetization M represents J_{pm}, the current density of the PMs [3]. The boundary conditions are applied to each material region to calculate the tangential and normal components of the magnetic flux density induced by the PMs. The governing equation given in (2) can be solved as follows:

$$B_{II}^{x}=\frac{\mu_0}{2}\sum_{n=1,3}^{\infty}\left(\frac{\sinh(nkh)}{\sin(nkg)}\right)\left(\frac{e^{nky}}{e^{nkg}}-\frac{e^{nkg}}{e^{nky}}\right)\cdot\frac{b_n}{nk}\cdot\sin(nkx) \qquad (6)$$

$$B_{II}^{y}=-\frac{\mu_0}{2}\sum_{n=1,3}^{\infty}\left(\frac{\sinh(nkh)}{\sin(nkg)}\right)\left(\frac{e^{nky}}{e^{nkg}}-\frac{e^{nkg}}{e^{nky}}\right)\cdot\frac{b_n}{nk}\cdot\cos(nkx) \qquad (7)$$

Fig. 2 shows the magnetic field due owing to an armature current with unexcited PMs. The governing equation for region II is as follows:

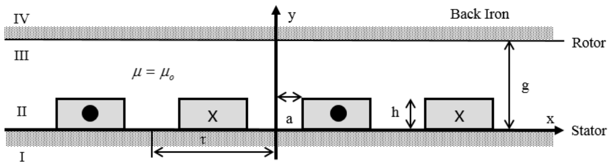

Fig. 2 Magnetic field due to armature current

$$\frac{\partial A(x,y)}{\partial x^2}+\frac{\partial A(x,y)}{\partial y^2}=-\mu_0 J(x) \qquad \text{Region II} \qquad (8)$$

By applying boundary conditions to each material region, the equations can be solved. These are as follows, where is $k=\pi/\tau$

$$B_{II}^{x}=\frac{\mu_0}{2}\sum_{n=1,3}^{\infty}\left(\frac{\sinh(nkh)}{\sin(nkg)}\right)\left(\frac{e^{nky}}{e^{nkg}}-\frac{e^{nkg}}{e^{nky}}\right)\cdot\frac{b_n}{nk}\cdot\sin(nkx) \qquad (9)$$

$$B_{II}^{y}=-\frac{\mu_0}{2}\sum_{n=1,3}^{\infty}\left(\frac{\sinh(nkh)}{\sin(nkg)}\right)\left(\frac{e^{nky}}{e^{nkg}}-\frac{e^{nkg}}{e^{nky}}\right)\cdot\frac{b_n}{nk}\cdot\cos(nkx) \qquad (10)$$

$$B_{III}^{x}=-\mu_0\sum_{n=1,3}^{\infty}\left(\frac{\sinh(nk(g-h))}{\sin(nkg)}\right)\sinh(nky)\cdot\frac{b_n}{nk}\cdot\sin(nkx) \qquad (11)$$

$$B_{III}^{y}=-\mu_0\sum_{n=1,3}^{\infty}\left(1-\frac{\sinh(nk(g-h))}{\sin(nkg)}\right)\cosh(nky)\cdot\frac{b_n}{nk}\cdot\cos(nkx) \qquad (12)$$

$$b_n=\frac{4J_0}{n\pi}\cdot\cos(nka) \qquad (13)$$

After all calculations are completed, the resultant magnetic field is calculated by using a superposed magnetic field generated by the PMs and the armature current.

2.2 Parameter Analysis

The Space Harmonic Analysis method is used to analyze the design parameters of the outer-rotor-type SPMSM. The specifications for the motor are listed in Table 1. The tendencies of the Phase Back_EMF, THD, and Cogging torque are analyzed according to changes in the pole angle. Fig. 3 shows the tendencies of these characteristics. Point * is selected from the design points of the initial model through a tendency analysis because Point * has enough Phase Back_EMF and a relatively small THD and Cogging torque.

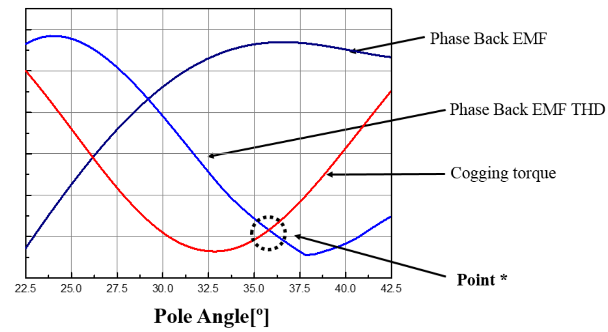

Fig. 3 Result of SHA

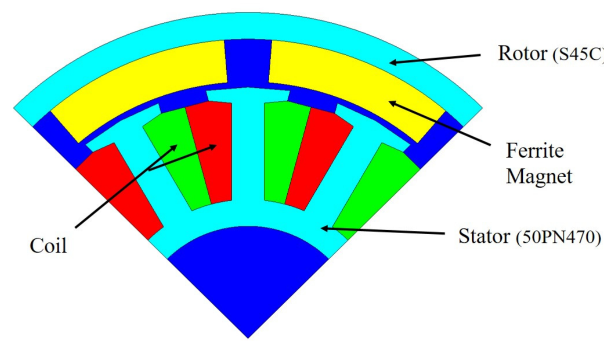

Fig. 4 Initial model

Table 2 The characteristic value of the initial model

Item	Value
Phase Back_EMF [V_{rms}]@1000rpm	1.169
THD [%] @1000rpm	5.27
Cogging torque [Nm]	0.160

2.3 Initial Design Result

Fig. 4 shows the designed initial configuration of the SPMSM. After modeling, FEA is used to verifying verify the characteristics. Table 2 shows the characteristic values of the initial model. Following the results, the value of the cogging torque is 0.16 Nm. This motor, for the CVVT, which operates at low speed and low torque, should have a small cogging torque for effective performance. Therefore, the cogging torque of the initial model must be reduced.

3. Optimum Design

3.1 Response Surface Methodology (RSM)

In this paper, the RSM, which is an optimum design method, is used [4]. RSM is a method of statistical analysis based on the values obtained in an experiment or simulation results of a reaction. RSM is used when k design variables affecting compositely to objective function η.

$$\eta = F(x_1, x_2, x_3, \ldots x_k) \tag{14}$$

In equation (14), the actual reaction function F is very complex to ascertain mathematically. Therefore a multiple regression model, which is assumed to react function, is used since it is a more practical and simple model for design variables. In this paper, Y, which is the approximate function for F, represents the second-order polynomial model based on a Taylor series. In general, the response model can be written as

$$Y = \beta_0 + \sum_{j=1}^{k} \beta_j x_j + \sum_{j=1}^{k} \beta_{jj} x_j^2 + \sum_{j=1}^{k} \sum_{j>i}^{k} \beta_{ij} x_i x_j + \varepsilon \tag{15}$$

where β represents the regression coefficients for the design variables, and ε is a random error that is treated as a statistical error. The observation response vector Y through n data points may be written using matrix notation as

$$\mathrm{Y} = \mathrm{X}\beta + \varepsilon \tag{16}$$

The least square method is used to estimate unknown vector β. The least square function L is

$$\mathrm{L} = \sum_{i=1}^{n} \varepsilon_i^2 = \varepsilon' \varepsilon = (\mathrm{Y} - \mathrm{X}\beta)'(\mathrm{Y} - \mathrm{X}\beta) \tag{17}$$

The estimated vector b through the least square method can be written as (18), and the fitted response vector Y is represented as follows (19):

$$\mathrm{b} = (\mathrm{X}^{\mathrm{T}}\mathrm{X})^{-1}\mathrm{X}^{\mathrm{T}} y \tag{18}$$

$$\mathrm{Y} = \mathrm{X}\mathrm{b} \tag{19}$$

In this paper, RSM is applied to create appropriate response models of the cogging torque. Central composite design (CCD) is employed as the experimental design method to estimate the fitted model of each response [5]. CCD consists of three parts: complete 2k factorial design points, axial points and center point There are a total of nine points in the relationship between the design variables, and the output is considered as k = 2.

$$NS_{CCD} = 2^k + 2 \cdot k + 1 \tag{20}$$

3.2 Optimum Model Design

The slot opening and eccentricity are chosen as the design variables for RSM because these values affect the cogging torque. Fig. 5 shows these two variables. Table 3 lists a range of RSM variables. For the range of the slot opening, the minimum value is twice the coil diameter (0.85 × 2 = 1.7 mm), and the maximum value is that of the initial model (4.5 mm). In the range of eccentricity, the minimum value is 1 mm, and the maximum value is 11 mm. This is a limiting value in manufacturing.

Table 3 The range of design variables

Factor	Min.	Max.
Slot opening [mm]	1.7	4.5
Eccentricity [mm]	1.0	11.0

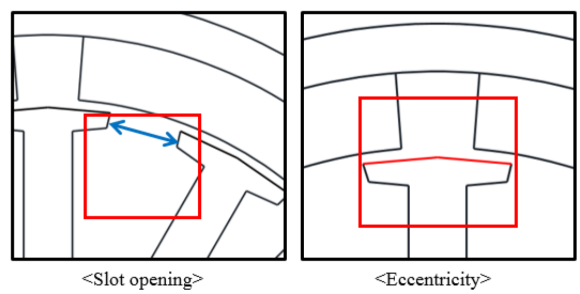

Fig. 5 Two design variables

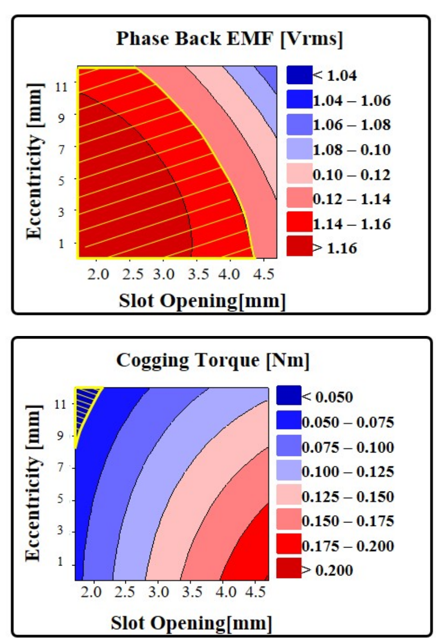

Fig. 6 Result plot of RSM

Through an analysis of the objective function, the optimum design values of the variables are determined. For the phase back EMF, both the slot opening and eccentricity are smaller, and the value of the phase back EMF is larger. On the other hand, the cogging torque decreases when the slot opening is smaller and the eccentricity is larger. The results of RSM contour plots are displayed in Fig. 6.

3.3 Optimum Design Result

As a result, a design area that has enough phase back EMF and a small cogging torque is selected. The results show that the optimum value of the slot opening and eccentricity are 1.7 mm and 11 mm, respectively. The slot opening and eccentricity of the initial model are 4.5 mm and 0 mm, respectively. The comparison between the initial model and optimum model is shown in Fig. 7.

FEA is used to verify the characteristics of the optimum design model. Fig. 8 and Table 4 show a comparison of the FEA results of for the phase back EMF and cogging torque of the initial model and optimized model.

Table 4 Result data

25℃	Phase Back_EMF @1000rpm [V]	THD [%]	Cogging torque [Nm]
Initial model	1.169	5.27	0.160
Optimum model	1.164	3.78	0.047

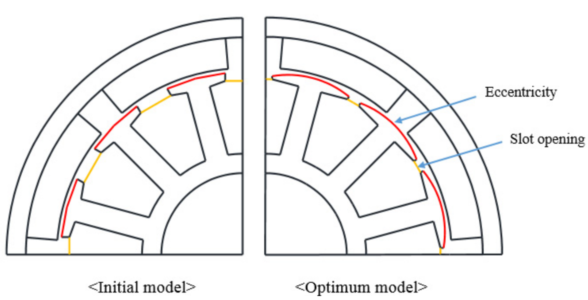

Fig. 7 Initial model and optimum model

4. Conclusion

In this paper, an outer-rotor-type SPMSM for a CVVT system is designed. For better performance of the CVVT system, a cogging-torque reduction process was conducted. An analytical method, SHA, was used to design an initial model of the outer-rotor-type SPMSM with a concentrated winding. After analyzing the characteristics of the initial model, the cogging-torque value of the initial model was

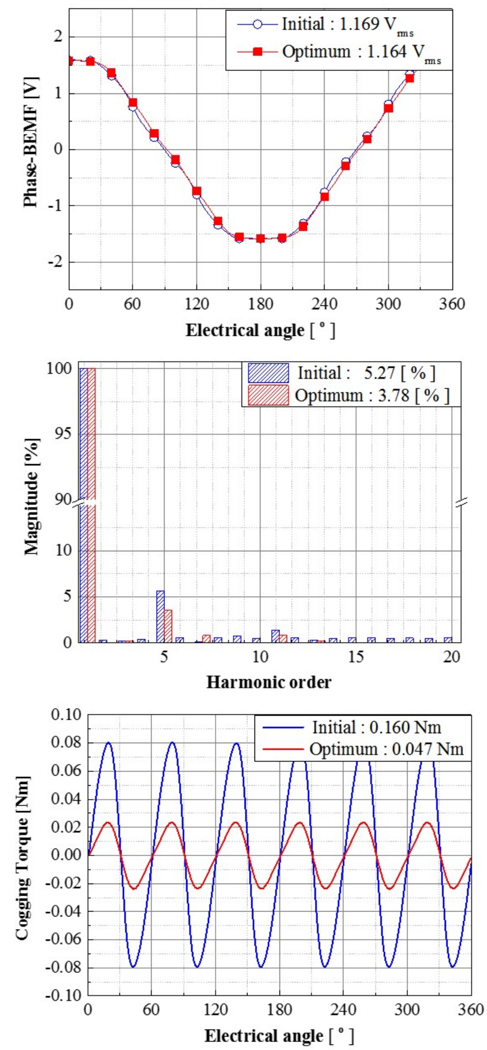

Fig. 8 FEA result

larger than the required standard. Therefore, an optimization method, RSM, was proposed to minimize the cogging torque. Two design factors (slot opening and eccentricity) were selected to reduce the cogging torque. Through RSM, the optimum values of the two design variables are selected. The performance of the optimum SPMSM was verified by FEA.

Acknowleedgments.

This research was supported by the MSIP(Ministry of Science, ICT and Future Planning), Korea, under the ITRC(Information Technology Research Center) support program(IITP-2016-H8601-16-1005) supervised by the IITP(Institute for Information & communications Technology Promotion).

References

[1] P. Barkan., and T. Dresner., “A Review of Variable Valve Timing Benefits and Modes of Operation“ SAE Technical Paper Series., paper 891678, 1989

[2] K. C. Lim., J. P. Hong., and G. T. Kim., “The Novel Technique Considering Slot Effect by Equivalent Magnetizing Current”, IEEE Transactions on Magnetics., pp. 3691-3693., 1998

[3] NADY BOULES., “Prediction of No-Load Flux Density Distribution in Permanent Magnet Machines”, IEEE Transactions on Industry Application., vol. IA-21, pp. 63-643., 1985

[4] S. I. Kim., J. Y. Lee., Y. K. Kim., J. P. Hong., Y. Hur., and Y.H. Jung., “Optimization for Reduction of Torque Ripple in Interior Permanent Magnet Motor by Using the Taguchi Method”, IEEE Transaction on Magnetics, Vol 41. pp. 1796-1779., 2005

[5] Raymond H. Myers., Douglas C. Montgomery., “Response Surface Methodology”, Process and Product Optimization Using Design Experiments, John Wiley & Sons., 1995

저 자 소 개

김 재 의(Jae-Yui Kim)

Jae-Yui Kim received the Bachelor's degree in mechanical engineering from Hanyang University, Seoul, Korea, in 2015. Currently he is working toward the Master's degree in automotive engineering. His research interests are design electric machines for automotive and industrial applications.

김 동 민(Dong-Min Kim)

Dong-Min Kim received Bachelor's degree in electronic information systems engineering from Hanyang University, Korea in 2013. Currently he is pursuing Ph.D. degree in automotive engineering from Hanyang University, Korea. His research interests are design and control of electric machine for automotive applications, and modeling of electric vehicles and hybrid electric vehicles.

박 수 환(Soo-Hwan Park)

Soo-Hwan Park received the Bachelor's degree in mechanical engineering from Hanyang University, Seoul, Korea, in 2014. He is currently working toward the Ph.D. degree in automotive engineering. His research interests are the electric machines for industrial applications and drive.

홍 정 표(Jung-Pyo Hong)

Jung-Pyo Hong received the Ph.D. degree in electrical engineering from Hanyang University, Korea, in 1995. Since 2006 he has been working as a professor in the Hanyang University, Korea. His research interests are the design of electric machines, optimization and numerical analysis of electromechanics.